Supporting Information

MOF Derived Two-dimensional N-doped Carbon Nanosheets Coupled with Co-Fe-P-Se as Efficient Bifunctional OER/ORR Catalysts

Hengbo Wu[a], Jie Wang[c], Ji Yan[d], Zexing Wu[b], *, Wei Jin[a, *]

a) School of Chemical and Material Engineering, Jiangnan University, Wuxi 214122, China

b) College of Chemistry and Molecular Engineering, Qingdao University of Science & Technology, Qingdao 266042, PR China

c) College of Chemistry and Pharmaceutical Sciences, Qingdao Agricultural University, Qingdao, 266109, China.

d) School of Materials and Chemical Engineering, Zhengzhou University of Light Industry, Zhengzhou 450001, Henan, PR China

Experimental section

Samples synthesis

Typically, $Co(NO_3)_2 \cdot 6H_2O$ and $FeCl_3 \cdot 6H_2O$ with different molar ratios (Co:Fe, 1:1, 1:3, 1:5) were dissolved in 10 mL ethanol solution (solution A). 1.4 g (10 mmol) of HMT was added into 10 mL ethanol and stirred to form clear solution (solution B). Then, solution A was mixed with solution B to form yellow-green precipitates immediately. The mixture solution was continually stirred for 10 h and the product was collected by vacuum filtration and dried at 60 ^oC (Co-Fe-HMT). Subsequently, the obtained Co-Fe-HMT frameworks (0.1g) were pyrolyzed in the presence of $NaH_2PO_2 \cdot H_2O$ and selenium powder at 600 °C for 2 h in nitrogen atmosphere, denoted as Co-Fe-P-Se/NC (Scheme 1). For comparison, other samples were synthesized using the identical strategy. Co/NC and Fe/NC were prepared in the absence of $FeCl_3 \cdot 6H_2O$ $NaH_2PO_2 \cdot H_2O$, selenium powder and $Co(NO_3)_2 \cdot 6H_2O$, $NaH_2PO_2 \cdot H_2O$, selenium powder, respectively. Co-Fe-Se/NC was synthesized without the addition of $NaH_2PO_2 \cdot H_2O$. Co-Fe-P/NC was synthesized without the addition of selenium powder. Co-P-Se/NC and Fe-P-Se/NC were prepared in the absence of $FeCl_3 \cdot 6H_2O$ and $Co(NO_3)_2 \cdot 6H_2O$, respectively

Physical Characterization

The surface morphology of the prepared samples were measured by field emission scanning electron microscopy (FE-SEM, Hitachi S4800) and transmission electron microscope (Tecnai G2 20) with an acceleration voltage of 200 kV. X-ray diffractometer (XRD, BUKER AXS D8) was performed to collect the structural information of the obtained samples. Elemental content and chemical valence state were collected by X-ray photoelectron spectroscopy (XPS, Thermo ESCALAB 250XI). Fourier transform infrared spectroscopy (FT-IR, WQF-600N) was used to study the chemical structures of the prepared nanomaterials.

Electrochemical Characterization

All the electrochemical measurements were carried out in a typical three-electrode system on a CHI760e electrochemical workstation by using glassy carbon electrode (5mm in diameter), graphite rod and Ag/AgCl as working electrode, counter electrode and reference electrode, respectively. 2 mg catalyst powder with 0.4 mg Vulcan XC-72 was dispersed in a mixture of 392 µL ethanol and 8 µL 5% Nafion by sonication for 1 h to from homogenous ink. Then 11.5 µL of the obtained ink was dropped onto polished glassy carbon electrode with loading amount of 0.35 mg cm^{-2} and dried at room temperature.

Electrochemical studies were performed by using cyclic voltammetry (CV) and linear sweep voltammetry (LSV) techniques at room temperature. All the LSVs for OER and ORR were collected with a scanning rate of 5 mV s^{-1}. Using the slopes of Koutecky-Levich (K-L) plots to calculate the electron transfer number (n) in an ORR process:

$$\frac{1}{j} = \frac{1}{jk} + \frac{1}{Bw^{1/2}} \quad (1)$$

$$B = 0.2FC_0D_0^{(2/3)}V^{(-1/6)} \quad (2)$$

where jk, j, w represent the kinetic current density at a constant potential, the measured current density, and the electrode rotating speed of the disk, respectively.F

is Faraday constant (96485 C/mol), C_0 is the bulk concentration of O_2 (1.2×10^{-6} mol/cm^2), D_0 is the diffusion coefficient of O_2 in 0.1 M KOH (1.9×10^{-5}cm^{-2}/s) and V is the kinematic viscosity of the electrolyte (0.01cm^2/s).

Zinc–air battery test

0.2 g of Co-Fe-P-Se/NC was dispersed in a mixture of 1.96 mL ethanol and 40 µL Nafion (5%) and ultra-sonicated to form homogenous ink. For Zn-air battery, a carbon paper electrode (1 cm^2) equipped with Co-Fe-P-Se/NC (10 mg) was used as cathode and a polished Zn foil as anode. The electrolyte was 6 M KOH with 0.2 M Zn $(CH_3COO)_2$. All Zn-air batteries were evaluated under ambient conditions. Constant current discharge-charge cycle is performed at room temperature in a LAND CT2001A battery system.

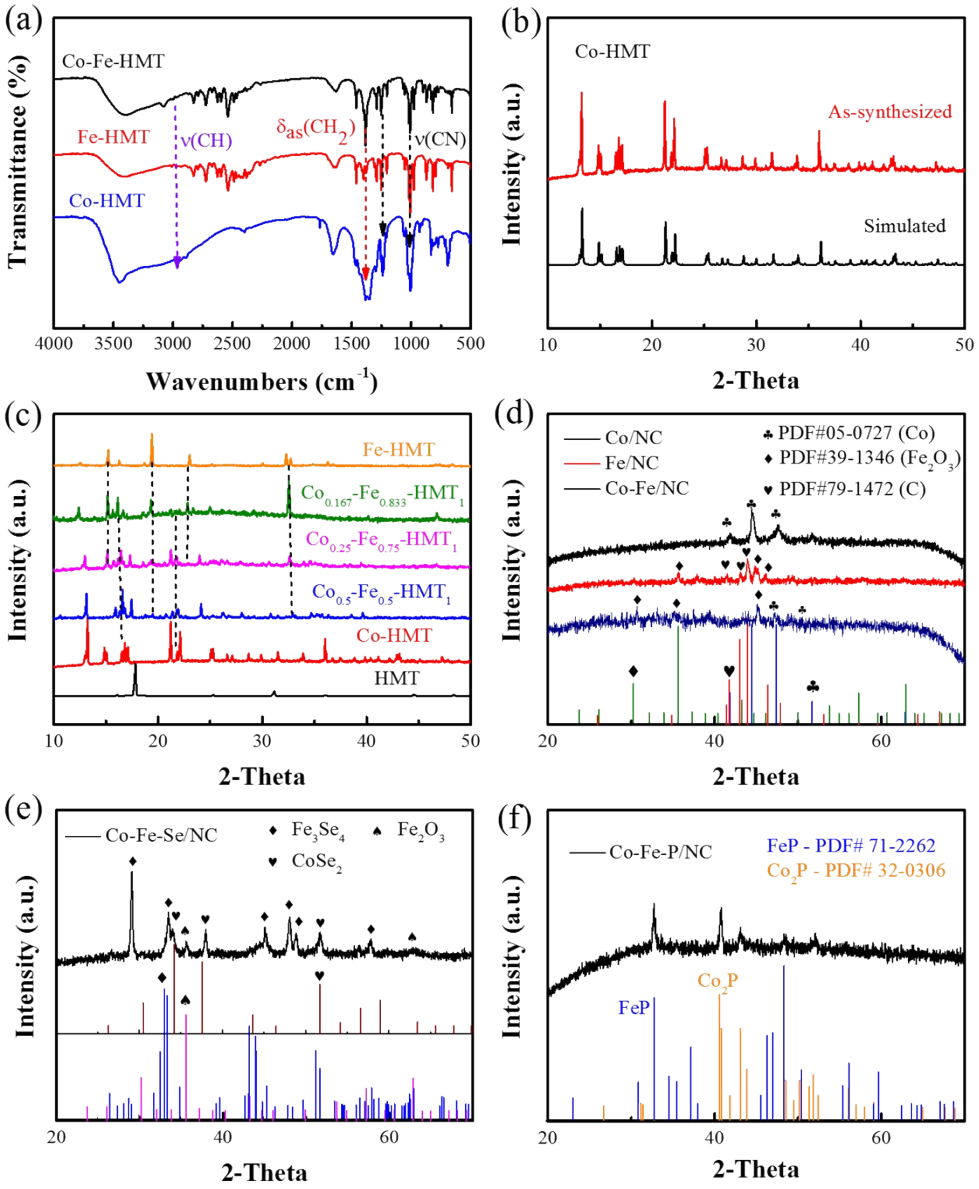

Fig. S1 (a) FT-IR spectrum of Co-HMT, Fe-HMT and Co-Fe-HMT. (b) Experimental and simulated powder XRD pattern of Co-HMT. (c)XRD patterns of HMT and Co-Fe-HMT nanorods with different molar ratios. (d) XRD pattern of Co/NC, Fe/NC and Co-Fe/NC. (e) XRD pattern of Co-Fe-Se/NC. (f) XRD pattern of Co-Fe-P/NC.

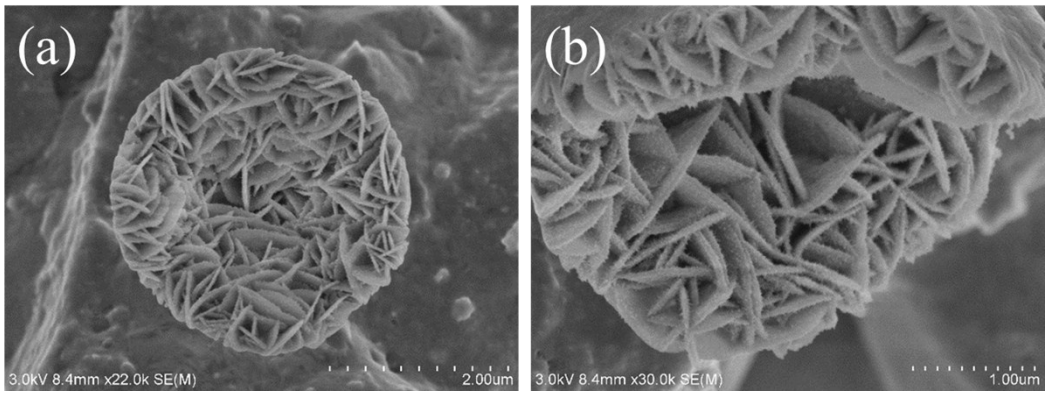

Fig. S2 FE-SEM image of the obtained Co-Fe/NC.

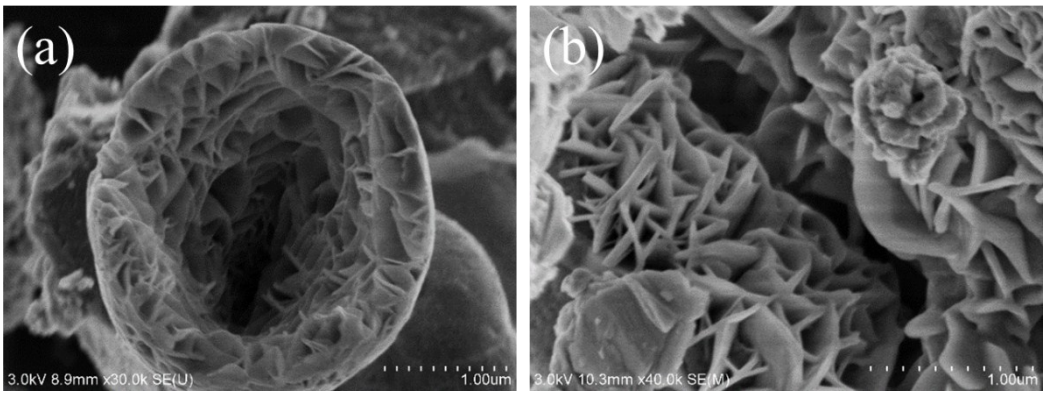

Fig. S3 FE-SEM image of the obtained Co-Fe-Se/NC.

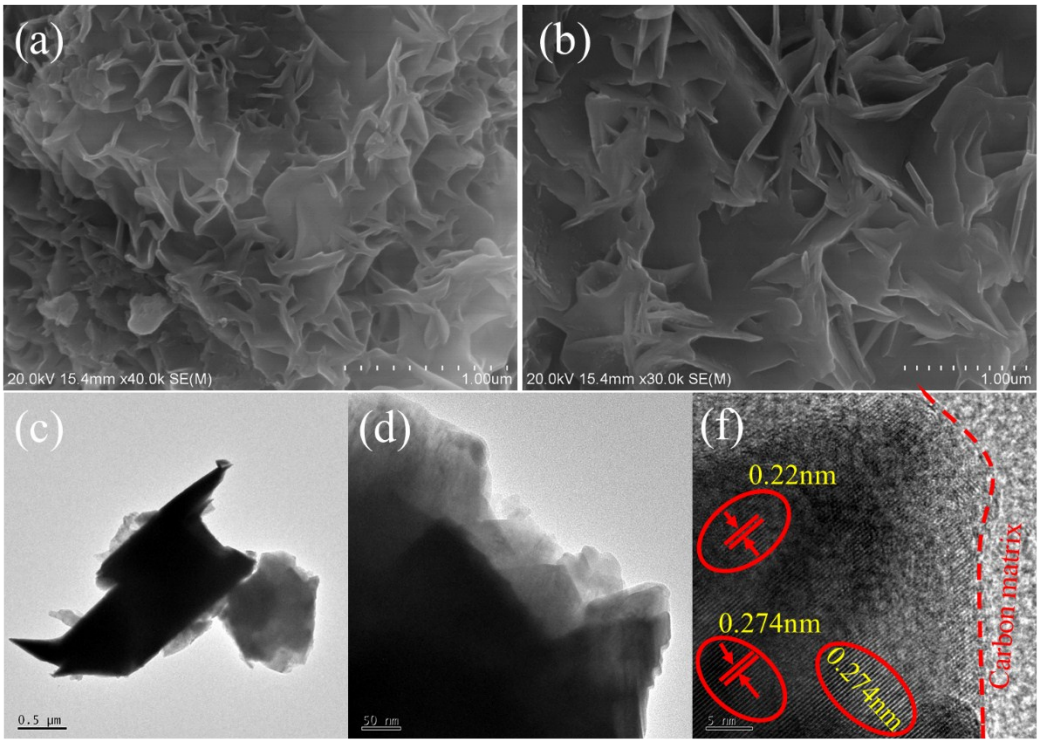

Fig. S4 FE-SEM (a -b). Low (c-d) and high resolution (f) TEM images of the obtained Co-Fe-P/NC.

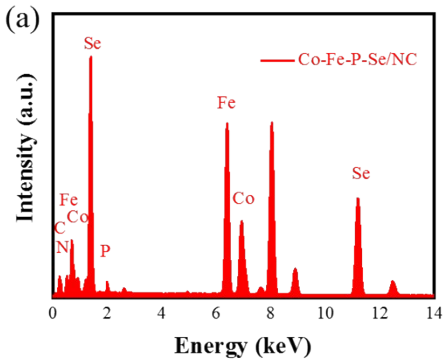

Fig. S5 (a) EDX spectra of Co-Fe-P-Se/NC.

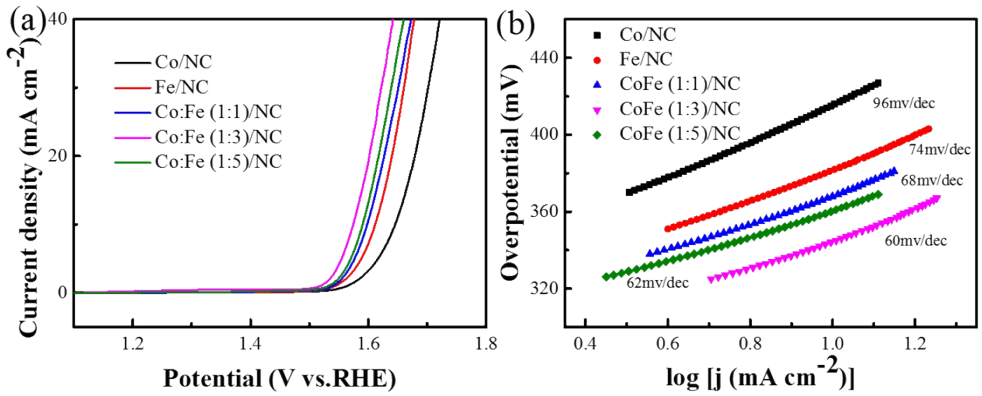

Fig. S6 (a) LSV polarization curves (b)The corresponding Tafel plots of Co/NC, Fe/NC, Co-Fe/NC with different ratios in OER process respectively.

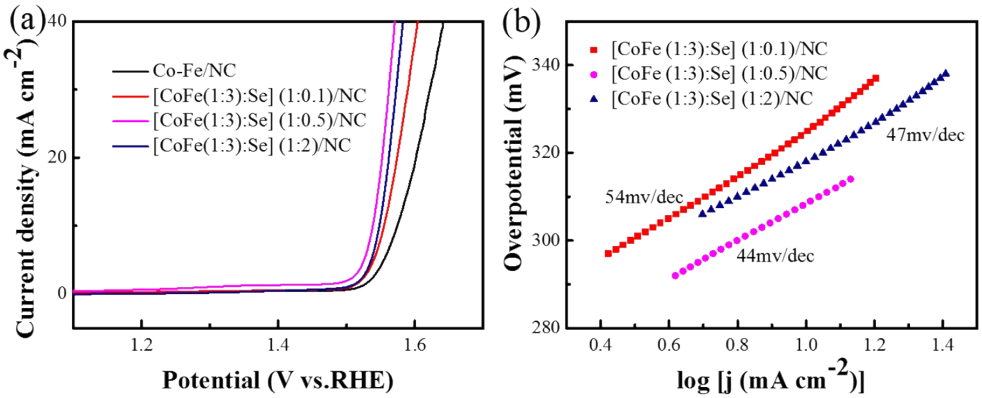

Fig. S7 (a) LSV polarization curves (b) The corresponding Tafel plots of Co-Fe/NC and Co-Fe-Se/NC with different ratios of Se in OER process respectively.

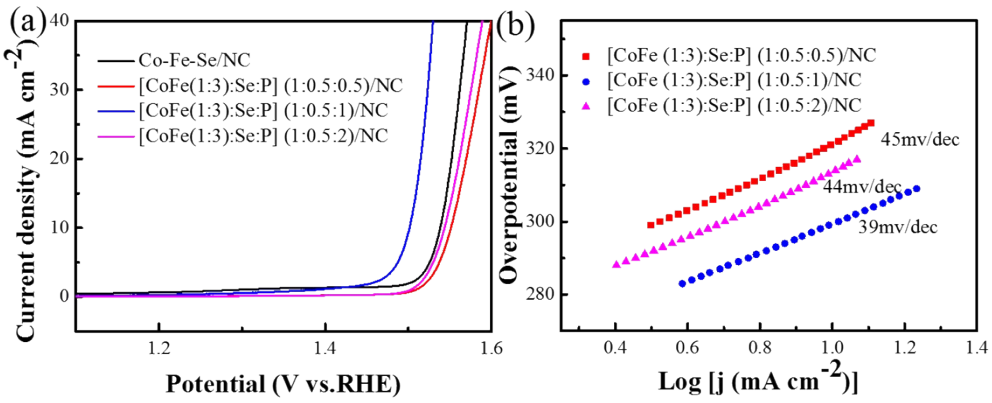

Fig. S8 (a) LSV polarization curves (b)The corresponding Tafel plots of Co-Fe-Se/NC and Co-Fe-P-Se/NC with different ratios of NaH_2PO_2 in OER process respectively.

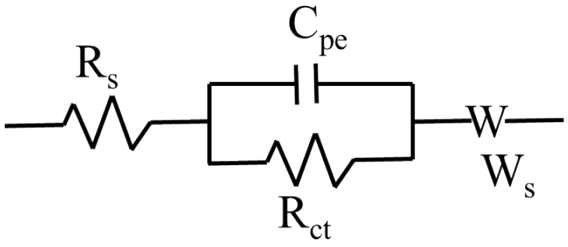

Fig. S9 equivalent circuit for the electrodes.

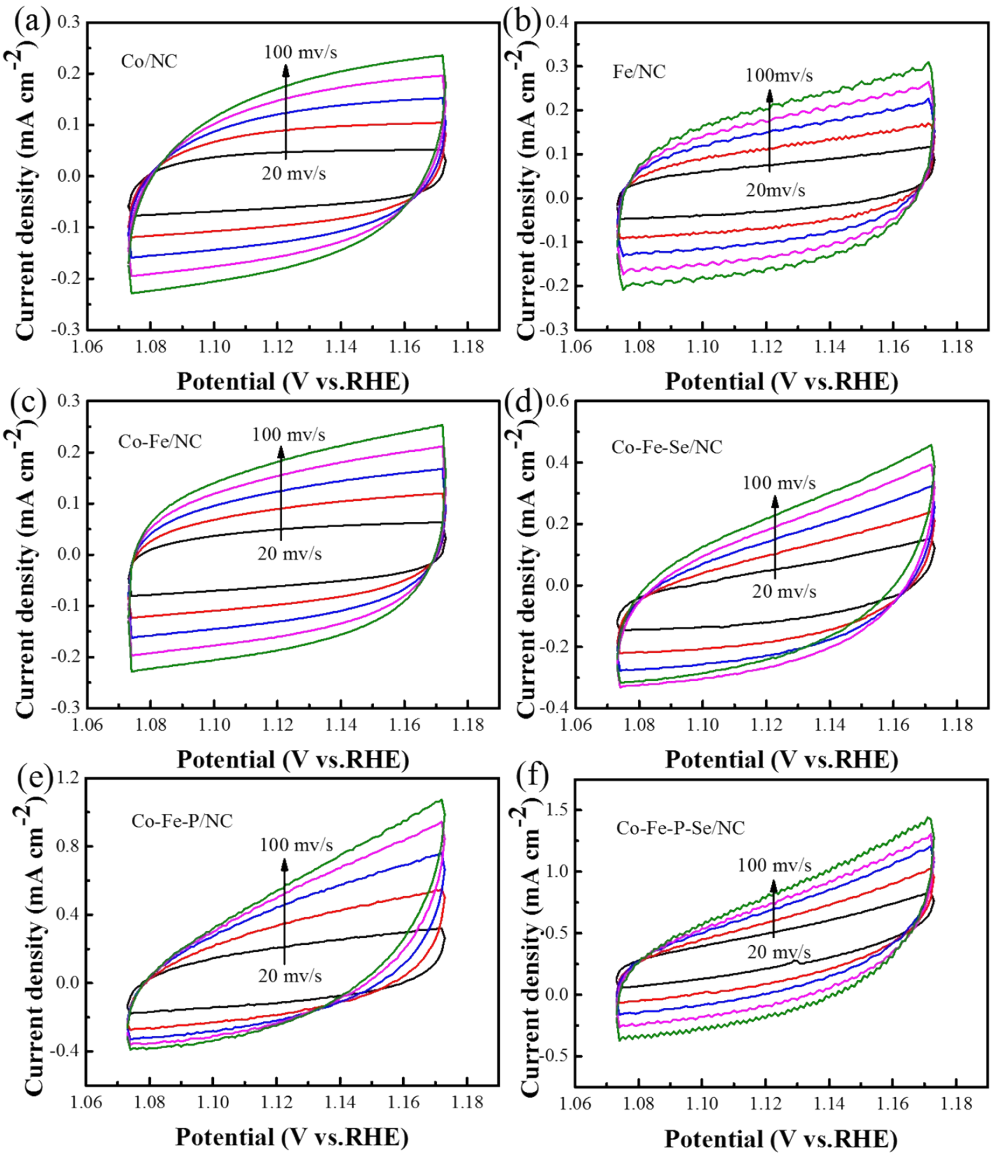

Fig. S10 CVs of Co/NC(a), Fe/NC(b), Co-Fe/NC(c), Co-Fe-Se/NC(d) , Co-Fe-P/NC(e) ,Co-Fe-P-Se/NC(f) at different sweeping rates from 20 mV s^{-1} to 100 mV s^{-1} in 1 M KOH.

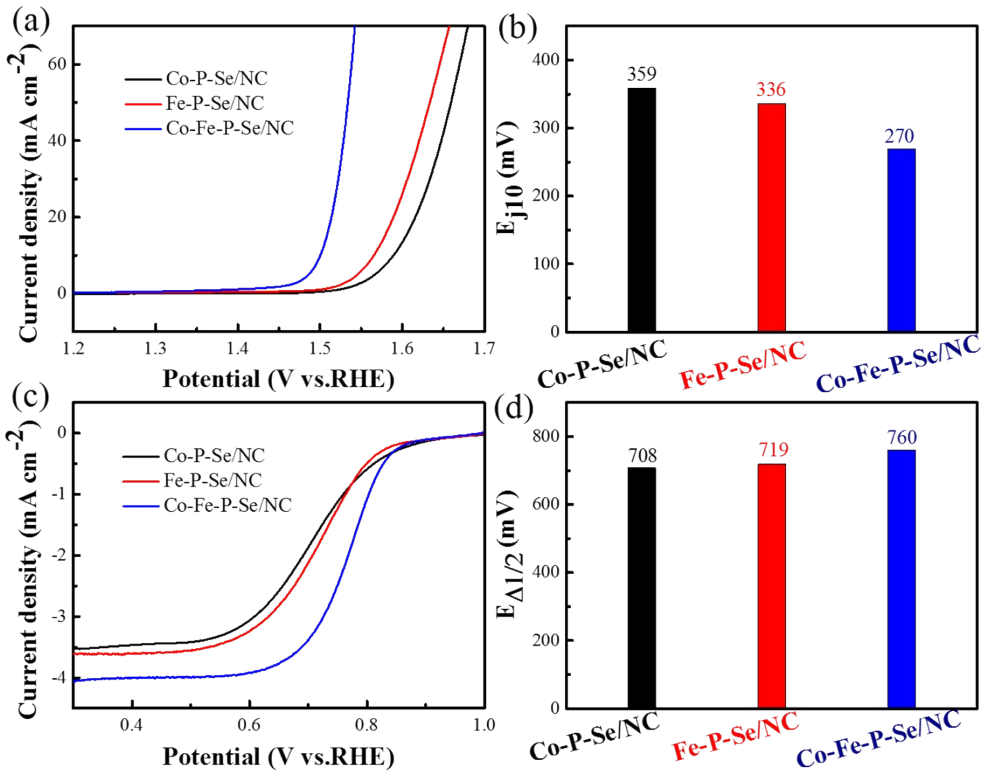

Fig. S11 LSVs of Co-P-Se/NC, Fe-P-Se/NC and Co-Fe-P-Se/NC for OER (a) and ORR (c). Overpotentials between the E_{j10} for OER (b) and $E_{1/2}$ for ORR (d) of the prepared samples.

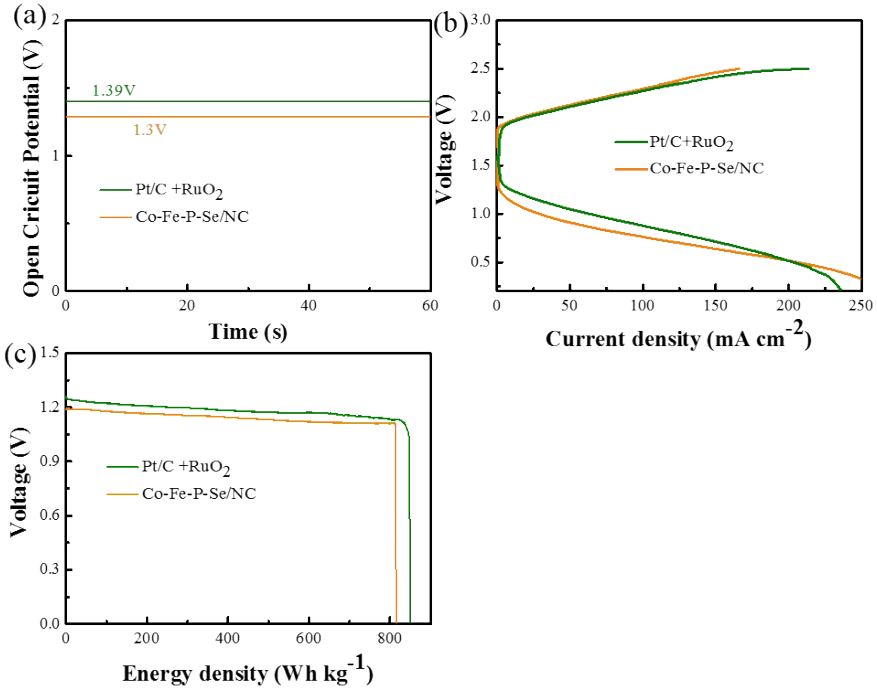

Fig. S12 Znic–air battery performance: (a) Open circuit plots (b) Charge and discharge polarization curves (c) the corresponding energy density plots at 10 mA cm^{-2}

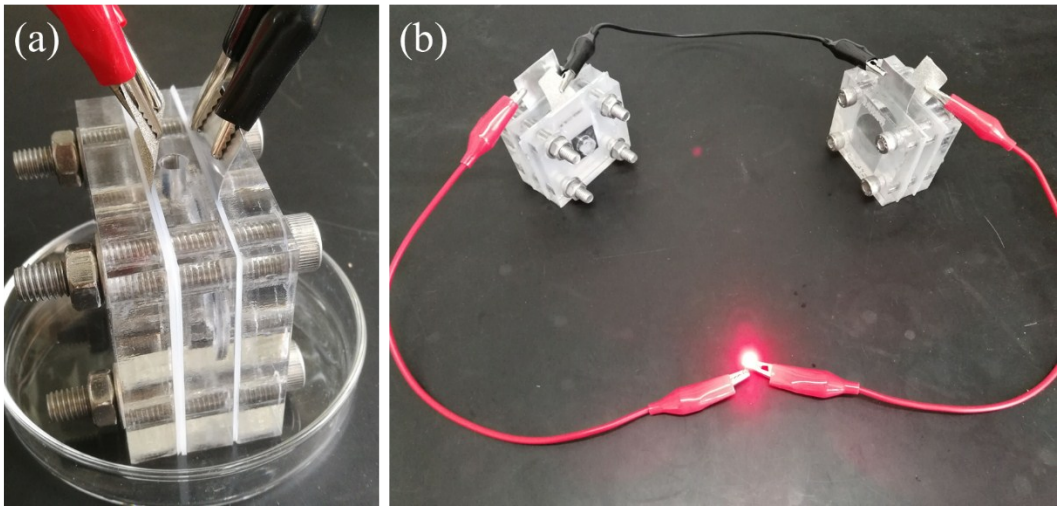

Fig. S13 (a) Schematic illustration of the Zinc–air batteries (b) photograph of a red LED (2.0 V) powered by two tandem Zinc-air batteries equipped with Co-Fe-P-Se/NC

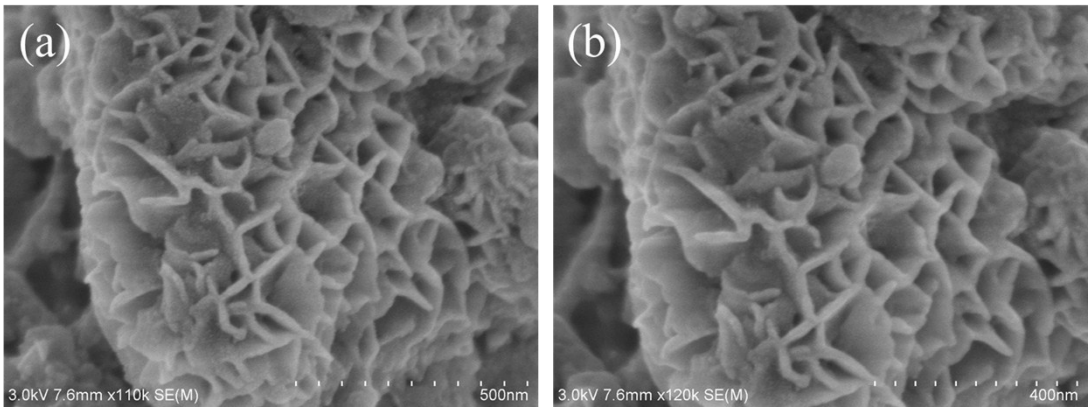

Fig. S14 (a, b) FE-SEM images of the obtained Co-Fe-P-Se/NC after zinc-air batteries test.

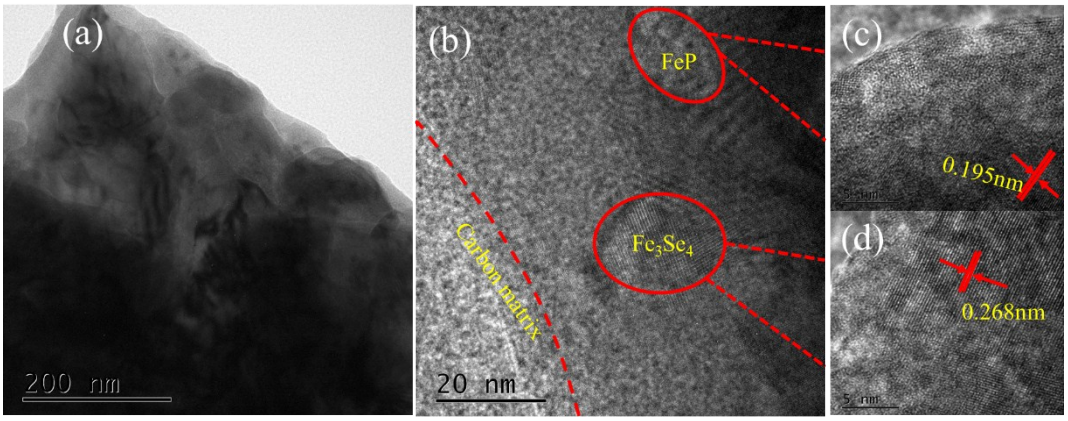

Fig. S15 HR-TEM image of the obtained Co-Fe-P-Se/NC after Zinc-air batteries test

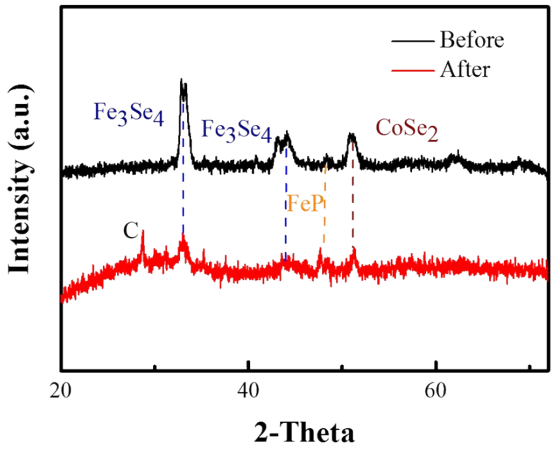

Fig. S16 XRD pattern of Co-Fe-P-Se/NC after stability test for Zinc-air batteries

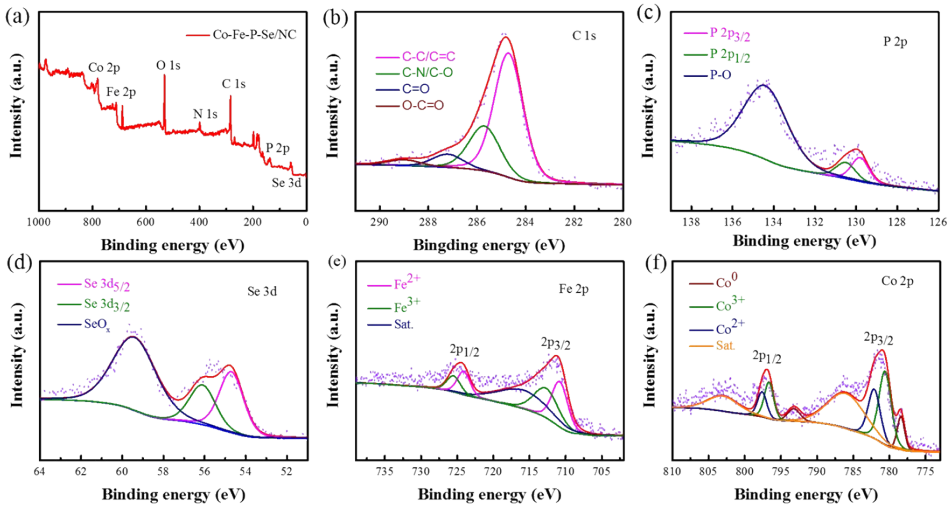

Fig. S17 (a) XPS spectra of Co-Fe-P-Se/NC after stability test for zinc-air batteries and corresponding C 1s(b), P 2p(c), Se 3d(d), Fe 2p(e) and Co 2p(f).

Table S1 Comparison of the R_s (Ω), R_{ct} (Ω) values of Co/NC, Fe/NC, Co-Fe/NC, Co-Fe-Se/NC , Co-Fe-P/NC, Co-Fe-P-Se/NC in alkaline media.

Catalyst	R_s (Ω)	R_{ct} (Ω)
Co/NC	3.669	12.1
Fe/NC	2.814	8.545
Co-Fe/NC	3.322	7.337
Co-Fe-Se/NC	3.153	5.66
Co-Fe-P/NC	4.549	5.162
Co-Fe-P-Se/NC	3.93	3.235

Table S2 Comparison of the performances of ZABs of our work and other reported catalysts.

Catalysts	Electrolyte	Power density (mW/cm^2)	Open-circuit voltage (V)	Long-term Stability (h)	Energy density ($Wh\ Kg^{-1}$)	Ref.
Co-Fe-P-Se/NC	6.0 M KOH + 0.2 M $Zn(Ac)_2$	104	1.3	40	805	This work
Pt/C+RuO_2	6.0 M KOH + 0.2 M $Zn(Ac)_2$	108.5	1.39	17	848	This work
FeCo-NC ps	6.0 M KOH + 0.2 M $Zn(Ac)_2$	242	1.43	155	922	1
$CoIn_2S_4$/S-rGO	6.0 M KOH + 0.2 M ZnCl2	133	1.42	50	951	2
Fe/Fe_3C@C	6.0 M KOH	101.3	1.37	99	764.5	3
Co-N-CNTs	6.0 M KOH + 0.2 M $Zn(Ac)_2$	101	1.365	15	-	4
Co_3O_4-doped Co/CoFe	6 M KOH	97	1.43	65	819	5
N-GCNT/FeCo	6.0 M KOH + 0.2 M $Zn(Ac)_2$	89.3	1.48	40	653.2	6
Mn_3O_4/O-CNT	6.0 M KOH + 0.2 M $ZnCl_2$	86.6	1.45	150	-	7
NiFe@NCX	6 M KOH	80	-	34	732.3	8
CoO NRs	6 M KOH	60.2	1.43	20	583.3	9

CoZn-NC-700	6.0 M KOH + 0.2 M ZnCl2	152	1.36	64	694	10
NPMC-1000	6.0 M KOH	55	1.48	240	835	11
NCN-1000-5	6.0 M KOH + 0.2 M $Zn(Ac)_2$	207	1.44	330	806	12
P,S-CNS	6.0 M KOH + 0.2 M $Zn(Ac)_2$	198	1.51	100	845	13
BHPC-950	6.0 M KOH	197	1.44	180	963	14
NGM-Co	6.0 M KOH + 0.2 M $ZnCl_2$	152	1.439	60	840	15
NCNF	6.0 M KOH + 0.2 M $Zn(Ac)_2$	185	1.48	83	838	16
CoNi@NCNT/NF	6.0 M KOH + 0.2 M $Zn(Ac)_2$	127	1.4	90	845	17
Ag-Cu on Ni foam	6.0 M KOH + 0.2 M $Zn(Ac)_2$	85.8	1.48	33	641	18
Cu-Co_2P @ 2D-NPC	6.0 M KOH + 0.2 M $ZnCl_2$	236.1	1.4	160	950	19
CoN_4/NG	6M KOH + 0.2M ZnO	115	1.51	100	671	20

References

1. J. Liu, T. He, Q. Wang, Z. Zhou, Y. Zhang, H. Wu, Q. Li, J. Zheng, Z. Sun, Y. Lei, J. Ma and Y. Zhang, *J. Mater. Chem. A*, 2019, **7**, 12451-12456.
2. G. Fu, J. Wang, Y. Chen, Y. Liu, Y. Tang, J. B. Goodenough and J.-M. Lee, *Adv. Energy Mater.*, 2018, **8**, 1802263.
3. Q. Wang, Y. Lei, Z. Chen, N. Wu, Y. Wang, B. Wang and Y. Wang, *J. Mater. Chem. A*, 2018, **6**, 516-526.
4. T. Wang, Z. Kou, S. Mu, J. Liu, D. He, I. S. Amiinu, W. Meng, K. Zhou, Z. Luo, S. Chaemchuen and F. Verpoort, *Adv. Funct. Mater.*, 2018, **28**, 1705048.
5. T. Li, Y. Lu, S. Zhao, Z. D. Gao and Y. Y. Song, *J. Mater. Chem. A*, 2018, **6**, 3730-3737.
6. C. Y. Su, H. Cheng, W. Li, Z. Q. Liu, N. Li, Z. Hou, F. Q. Bai, H. X. Zhang and T. Y. Ma, *Adv. Energy Mater.*, 2017, **7**, 1602420.
7. L. Li, J. Yang, H. Yang, L. Zhang, J. Shao, W. Huang, B. Liu and X. Dong, *ACS Appl. Energy Mater.*, 2018, **1**, 963-969.
8. J. Zhu, M. Xiao, Y. Zhang, Z. Jin, Z. Peng, C. Liu, S. Chen, J. Ge and W. Xing, *ACS Catal.*, 2016, **6**, 6335-6342.
9. P. Da, M. Wu, K. Qiu, D. Yan, Y. Li, J. Mao, C. Dong, T. Ling and S. Qiao, *Chem. Eng. Sci.*, 2019, **194**, 127-133.
10. X. Wu, X. Han, X. Ma, W. Zhang, Y. Deng, C. Zhong and W. Hu, *ACS Appl. Mater. Interfaces*, 2017, **9**, 12574-12583.
11. J. Zhang, Z. Zhao, Z. Xia and L. Dai, *Nat. Nanotechnol.*, 2015, **10**, 444-452.
12. H. Jiang, J. Gu, X. Zheng, M. Liu, X. Qiu, L. Wang, W. Li, Z. Chen, X. Ji and J. Li, *Energy Environ. Sci.*, 2019, **12**, 322-333.
13. S. S. Shinde, C. H. Lee, A. Sami, D. H. Kim, S. U. Lee and J. H. Lee, *ACS nano*, 2017, **11**, 347-357.
14. M. Yang, X. Hu, Z. Fang, L. Sun, Z. Yuan, S. Wang, W. Hong, X. Chen and D. Yu, *Adv. Funct. Mater.*, 2017, **27**, 1701971.
15. C. Tang, B. Wang, H. F. Wang and Q. Zhang, *Adv. Mater.*, 2017, **29,** 1703185.
16. Q. Liu, Y. Wang, L. Dai and J. Yao, *Adv. Mater.*, 2016, **28**, 3000-3006.
17. W. Niu, S. Pakhira, K. Marcus, Z. Li, J. L. Mendoza-Cortes and Y. Yang, *Adv. Energy Mater.*, 2018, **8**, 1800480.
18. Y. Jin and F. Chen, *Electrochim. Acta*, 2015, **158**, 437-445.

19. L. Diao, T. Yang, B. Chen, B. Zhang, N. Zhao, C. Shi, E. Liu, L. Ma and C. He, *J. Mater. Chem. A*, 2019, **7**, 21232-21243.
20. L. Yang, L. Shi, D. Wang, Y. Lv and D. Cao, *Nano Energy*, 2018, **50**, 691-698.